

# Provable Unrestricted Adversarial Training without Compromise with Generalizability

Lilin Zhang, Ning Yang, Yanchao Sun, Philip S. Yu, *Fellow, IEEE*

**Abstract**—Adversarial training (AT) is widely considered as the most promising strategy to defend against adversarial attacks and has drawn increasing interest from researchers. However, the existing AT methods still suffer from two challenges. First, they are unable to handle unrestricted adversarial examples (UAEs), which are built from scratch, as opposed to restricted adversarial examples (RAEs), which are created by adding perturbations bound by an  $l_p$  norm to observed examples. Second, the existing AT methods often achieve adversarial robustness at the expense of standard generalizability (i.e., the accuracy on natural examples) because they make a tradeoff between them. To overcome these challenges, we propose a unique viewpoint that understands UAEs as imperceptibly perturbed unobserved examples. Also, we find that the tradeoff results from the separation of the distributions of adversarial examples and natural examples. Based on these ideas, we propose a novel AT approach called Provable Unrestricted Adversarial Training (PUAT), which can provide a target classifier with comprehensive adversarial robustness against both UAE and RAE, and simultaneously improve its standard generalizability. Particularly, PUAT utilizes partially labeled data to achieve effective UAE generation by accurately capturing the natural data distribution through a novel augmented triple-GAN. At the same time, PUAT extends the traditional AT by introducing the supervised loss of the target classifier into the adversarial loss and achieves the alignment between the UAE distribution, the natural data distribution, and the distribution learned by the classifier, with the collaboration of the augmented triple-GAN. Finally, the solid theoretical analysis and extensive experiments conducted on widely-used benchmarks demonstrate the superiority of PUAT.

**Index Terms**—Adversarial Robustness, Adversarial Training, Unrestricted Adversarial Examples, Standard Generalizability.

## 1 INTRODUCTION

DEEP neural network (DNN) has achieved groundbreaking success in a number of artificial intelligence application areas, including computer vision, object identification, and natural language processing, among others. Despite the remarkable success of DNN, seminal researches reveal its vulnerability to **adversarial examples** (AEs), which are inputs with non-random perturbations unnoticeable to humans but intentionally meant to cause victim models to deliver false outputs [1], [2], [3], [4]. The harms brought on by AEs have prompted ongoing efforts to increase DNN’s **adversarial robustness** (i.e., the accuracy on AEs), among which **adversarial training** (AT) has been largely acknowledged as the most promising defensive strategy [5], [6], [7].

The fundamental idea of AT was first proposed by Szegedy *et al.* [2], which adds AEs to the training set and uses a min-max game to create a robust classifier that can withstand worst-case attacks. In particular, AT alternately maximizes an adversarial loss incurred by AEs that are purposefully crafted using adversarial attacking methods such as FGSM [8] and PGD [9], and minimizes it by adjusting the target classifier’s parameters via a regular supervised training on the augmented training set. Numerous works have suggested strengthening the basic AT in order to increase adversarial robustness [10], [11], [12], [13], [14], [15].

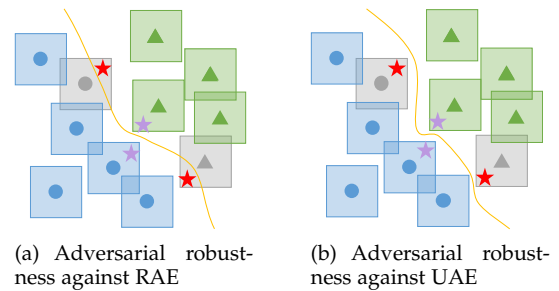


Fig. 1. Illustration of adversarial robustness against RAE and UAE. The blue dots and green triangles represent two classes of observed examples, respectively, and the gray ones represent the unobserved examples of the two classes. Each example is surrounded by a box representing its neighborhood with small distance. The purple stars represent RAEs while the red stars UAEs. The yellow curves are decision boundaries obtained by adversarial training.

Although the existing AT approaches have advanced significantly, we argue that the problem of adversarial robustness is still far from being well solved partly due to the following two challenges.

The issue of *Unrestricted Adversarial Example* (UAE) is the first obstacle. As previously mentioned, AT is conducted on a training set that includes AEs. However, the conventional AT approaches are frequently limited to perturbation-based AEs, which are created by adding adversarial perturbations with magnitudes restricted by an  $l_p$  norm to observed natural examples. We refer to such kind of AEs as restricted AE (RAE). In fact, RAEs only account for a small portion of possible AEs in real world. Recent works reveal the existence of UAEs, which are dissimilar to any observable example since they are built from scratch rather than by perturbing

- Lilin Zhang is with the School of Computer Science, Sichuan University, China. E-mail: zhanglilin@stu.scu.edu.cn
- Ning Yang is the corresponding author and with the School of Computer Science, Sichuan University, China. E-mail: yangning@scu.edu.cn
- Yanchao Sun is with the Department of Computer Science, University of Maryland, College Park, USA. E-mail: ycs@umd.edu
- Philip S. Yu is with the Department of Computer Science, University of Illinois at Chicago, USA. E-mail: psyu@uic.edu

existing examples [16], [17], [18], [19], [20]. Figure 1 provides an illustration showing how UAEs (represented by the red stars) are not the neighbors of any observed example (blue circle or green triangle), in contrast to RAEs (shown by the purple stars). Despite the adversarial robustness against RAE provided by conventional AT approaches, as seen in Figure 1(a), the classifier (with the yellow curve as the decision boundary) can still be deceived by UAEs because they also appear natural [16]. UAEs are more numerous, more covert, and more dangerous than RAEs since UAEs are not dependent on observed examples which are typically sparse. However, the existing works on UAE mainly focus on the generation of UAEs, which suffer from two defects. First, no explanation for why UAEs exist and why they are imperceptible to humans is provided in the existing works. Second, adversarial robustness against UAE still remains largely unexplored. Therefore, we need a new AT method that is able to offer the robustness against both UAE and RAE, which we refer to as **comprehensive adversarial robustness**. As shown in Figure 1(b), the classifier with comprehensive adversarial robustness is able to correctly predict the labels of both the UAEs and the RAEs.

The second challenge faced by the current AT approaches is the problem of the *deterioration of standard generalizability* (i.e., the accuracy on natural/natural testing examples). Early researches show that the standard generalizability of a classifier is sacrificed in order for conventional AT approaches to obtain the adversarial robustness for the classifier [9]. Zhang *et al.* [21] further demonstrate the existence of an upper-bound of the standard generalizability given the adversarial robustness, and Attias *et al.* [22] suggest lowering the upper-bound by increasing sample complexity. However, recent studies argue that the tradeoff may not be inevitable, and adversarial robustness and standard generalizability can coexist without negatively affecting each other [15], [23], [24], [25]. For example, Stutz *et al.* [15] demonstrate that the adversarial robustness against the AEs existing on the manifold of natural examples will equivalently lead to better generalization. Song *et al.* [24] and Xing *et al.* [25] propose to improve the standard generalizability by introducing robust local features and  $l_1$  penalty to AT, respectively. The existing efforts, however, only concentrate on RAEs. It is yet unknown that if and how the comprehensive adversarial robustness and the standard generalizability can both be improved simultaneously.

To address the first challenge, in this paper, we propose a *unique viewpoint that understands UAEs as imperceptibly perturbed unobserved examples* (gray dot or triangle in Figure 1), which logically explains why UAEs are dissimilar to observed examples and why UAEs can fool a classifier without confusing humans. Essentially, RAE can be thought of as a special UAE resulting from perturbing observed examples. If we generalize the concept of UAE to imperceptibly perturbed natural examples, regardless of whether they are observable, then *UAE can be regarded as a general form of AE*, which makes it feasible to provide comprehensive adversarial robustness.

For the second challenge, we find that the tradeoff exists because the target classifier can not generalize over two separated distributions, the AE distribution and the natural example distribution, and the distribution learned by the

classifier is a mix of them. Therefore, if we can align the distributions of UAEs and natural examples with the distribution learned by the target classifier, then the classifier can generalize over UAEs and natural examples without conflict, and we can expect to eliminate the tradeoff between comprehensive adversarial robustness and standard generalization and achieve a simultaneous improvement of both.

Based on these ideas, we propose a novel AT method called Provable Unrestricted Adversarial Training (PUAT), which *integrates the generation of UAEs and an extended AT on UAEs with a GAN-based framework, so that the distributions of UAEs and natural examples can be aligned with the distribution learned by the target classifier for simultaneously improving its comprehensive adversarial robustness and standard generalizability*. At first, we design a UAE generation module consisting of an attacker  $A$  and a conditional generator  $G$ , treating a UAE as an adversarially perturbed natural example. Different from the existing generative models for AEs, which often result in suboptimal AEs due to the gradient conflicts during the single optimization for both imperceptibility and harmfulness of AEs, our UAE generation module decouples the optimizations of imperceptibility and harmfulness of UAEs. Particularly,  $A$  is in charge of producing an adversarial perturbation that can fool the classifier, based on which  $G$  will generate a UAE for a certain class, which is equivalent to perturbing a natural example. PUAT ensures the imperceptibility of UAEs by aligning the UAE distribution learned by  $G$  with the natural example distribution via a G-C-D GAN, in contrast to conventional AT approaches that accomplish imperceptibility by an explicit norm constraint on the perturbations. The G-C-D GAN is a novel augmented triple-GAN that combines two conditional GANs: the G-D GAN, which consists of  $G$  and a discriminator  $D$ , and the C-D GAN, which consists of the target classifier  $C$  and  $D$ . Different from the original triple-GAN proposed by Li *et al.* [26], in G-C-D GAN the generator  $G$  is shared with the UAE generation module, which augments the input of  $G$  with the output of the attacker  $A$  and consequently allows  $G$  to draw UAEs from the UAE distribution. To facilitate the distributional alignment, we also make use of unlabeled data to create pseudo-labeled data for the training of G-C-D GAN since labeled data are usually insufficient for capturing the real data distribution. By leveraging partially labeled data, G-D GAN and C-D GAN can cooperate to help  $G$  capture the natural data distribution and the UAE generation module understand how to build a legitimate AE for a certain class.

In order to simultaneously improve the target classifier's comprehensive adversarial robustness and standard generalizability, PUAT conducts an extended AT between the target classifier  $C$  and the attacker  $A$ , which incorporates a supervised loss of the target classifier with the adversarial loss. The extended AT together with the G-C-D GAN leads to the alignment between the UAE distribution, the natural example distribution, and the distribution learned by  $C$ , which enables  $C$  to generalize without conflict on UAEs and natural examples. Finally, we theoretically and empirically demonstrate that PUAT realizes a consistent optimization for both the comprehensive adversarial robustness and the standard generalizability, eliminating the tradeoff between them and resulting in their mutual advantage. Our contri-

butions can be summarized as follows:

- We propose a unique viewpoint that understands UAEs as imperceptibly perturbed unobserved examples, which offers a logical and demonstrable explanation for UAEs’ discrepancies from observed examples, imperceptibility to humans, and the feasibility of comprehensive adversarial robustness against both RAE and UAE.
- We propose a novel AT approach called Provable Unrestricted Adversarial Training (PUAT), which, with theoretical guarantee, can simultaneously increase a classifier’s comprehensive adversarial robustness and standard generalizability through a distributional alignment.
- We provide a solid theoretical analysis to demonstrate that PUAT can eliminate the tradeoff between the comprehensive adversarial robustness and the standard generalizability through the distributional alignment.
- The extensive experiments conducted on widely adopted benchmarks verify the superiority of PUAT.

## 2 PRELIMINARIES AND PROBLEM FORMULATION

In this section, we first give the formal definition of UAE, then present our understanding of UAEs, and finally, formulate the AT on UAEs.

### 2.1 Definition of UAE

Let  $x \in \mathcal{X}$  and  $y \in \mathcal{Y}$  be an example and a label, respectively, where  $\mathcal{X}$  represents the data space with distribution  $P(x)$  while  $\mathcal{Y}$  the label space with distribution  $P(y)$ . Let  $o(\cdot) : \mathcal{O} \subseteq \mathcal{X} \rightarrow \mathcal{Y}$  be an oracle which is defined on its domain  $\mathcal{O}$  and tells the true label of an example  $x \in \mathcal{O}$ . Usually, the oracle  $o$  corresponds to humans and  $\mathcal{O}$  consists of all the examples that look natural to and can not confuse humans. Let  $C(\cdot) : \mathcal{X} \rightarrow \mathcal{Y}$  be the target classifier. Following the idea of [16], we define UAE as follow:

**Definition 1 (UAE).** For a well-trained classifier  $C$ , an example  $\tilde{x}$  with label  $y = o(\tilde{x})$  is an unrestricted adversarial example if  $\tilde{x} \sim P(x|y)$  and  $C(\tilde{x}) \neq y$ , where  $P(x|y)$  is the class likelihood.

### 2.2 Understanding of UAE

From Definition 1 we can see that similar to RAE, the harmfulness of a UAE is still defined by its ability to fool the classifier, i.e.,  $C(\tilde{x}) \neq y$ . But in contrast to RAE, the imperceptibility of a UAE is due to its capability of being drawn from the realistic distribution ( $\tilde{x} \sim P(x|y)$ ) rather than a norm-constraint. However, it is challenging how to enforce both imperceptibility and harmfulness for UAE. For this purpose, we understand UAE from the viewpoint of imperceptibly perturbed unobserved examples. In particular, for a natural example  $x \sim P(x|y)$ , there exists a perturbation  $z_a$  satisfying the imperceptibility  $\tilde{x} = G(x, z_a) \sim P(x|y)$ , and the harmfulness  $C(\tilde{x}) \neq y$ , where  $G$  is a learnable generative function. Obviously,  $G$  can be non-linear and the perturbation  $z_a$  is not necessarily additive. Following this idea, we can generate a UAE through two steps: drawing natural example and generating appropriate perturbation for it. It is noteworthy that such understanding brings the advantage that RAE can be viewed as a special UAE and UAEs are a superset of RAEs, thus enabling the adversarial robustness against UAEs to cover RAEs.

## 2.3 Adversarial Training on UAEs

To offer the comprehensive adversarial robustness to the target classifier, we want to conduct adversarial training on UAEs, which is defined as the following min-max game:

$$\min_C \max_A \mathcal{L}_{adv} = \frac{1}{|\mathcal{A}|} \sum_{(\tilde{x}_g, y_g) \in \mathcal{A}} \mathcal{L}_c(\tilde{x}_g, y_g), \quad (1)$$

where  $\mathcal{L}_{adv}$  is the adversarial loss,  $\mathcal{L}_c(x, y)$  is a loss function of the target classifier, e.g., cross-entropy,  $\mathcal{A}$  is a labeled UAE set, and  $\tilde{x}_g$  is a generated UAE with label  $y_g$ . In Equation (1), the inner maximization seeks the most harmful UAE set  $\mathcal{A}$  resulting in the poorest performance of the target classifier, while the outer minimization aims at adjusting the target classifier to reduce its sensitivity to UAEs. It is noteworthy that unlike traditional AT where AEs are searched explicitly with respect to a norm-constraint, the AT on UAEs defined by Equation (1) does not tell us how to find out the qualified UAEs that can reconcile the adversarial robustness and standard generalizability of the target classifier, which is another key challenge we want to address in this paper.

## 3 PROPOSED METHOD

In this section, we first give an overview of our Provable Unrestricted Adversarial Training (PUAT) model, and then describe its components and learning procedure in detail.

### 3.1 Overview of PUAT

As shown in Figure 2, PUAT consists of four components, an attacker  $A$ , a conditional generator  $G$ , a discriminator  $D$  and the target classifier  $C$ .  $A$  and  $G$  constitute the UAE generation module. According to our idea that a UAE can be regarded as the perturbed version of an unobserved natural example, we first use  $G$  to produce a labeled example  $(x_g, y_g) \sim P_G(x, y)$  representing an unobserved natural example, where  $P_G(x, y)$  is the distribution of the data-label pairs generated by  $G$  and the randomness stems from a white noise  $z$ . Then we invoke  $A$  and  $G$  to generate its perturbed version  $(\tilde{x}_g, y_g)$  as a UAE, where the perturbation  $z_a$  is produced by  $A$  based on the same  $z$ . To ensure the **harmfulness** of the UAEs, PUAT will try to adjust  $A$  via the AT between  $A$  and  $C$  so that the generated UAEs can fool the target classifier  $C$ , i.e.  $C(\tilde{x}_g) \neq y_g$ . Thus the UAEs follow the conditional distribution  $P_G(x, y|C(x) \neq y)$ . At the same time, to ensure the **imperceptibility** of the generated UAEs, we want to align the distribution  $P_G(x, y)$  with the true data distribution  $P(x, y)$ . For this purpose, we introduce a discriminator  $D$  to distinguish the examples  $\{(x_g, y_g)\}$ , which includes the UAEs  $\{(\tilde{x}_g, y_g)\}$ , from the true labeled examples  $\{(x_l, y_l) \sim P(x, y)\}$ , which together with  $G$  constitutes a class-conditional GAN, called G-D GAN. The optimization of the G-D GAN will adjust  $G$  so that the distribution  $P_G(x, y)$  converges to  $P(x, y)$ . The alignment of  $P_G(x, y)$  and the true data distribution  $P(x, y)$  will make a UAE drawn from  $P_G(x, y)$  look like a natural example, which results in the imperceptibility of UAEs.

However, in traditional conditional GAN, the discriminator  $D$  also plays the role to predict the class label of  $x_g$ , for which the optimization objective conflicts with that for distinguishing  $\{(x_g, y_g)\}$  from  $\{(x_l, y_l)\}$ . Such conflict will

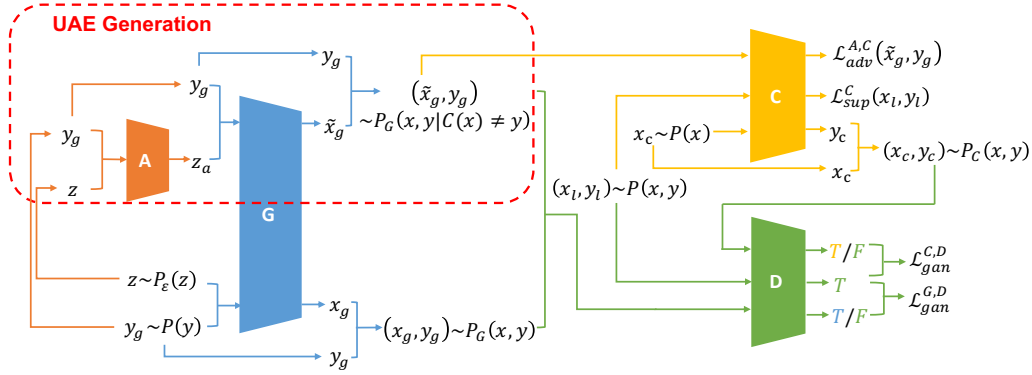


Fig. 2. Architecture of PUAT. The attacker  $A$  seeks the perturbation  $z_a$ , and the generator  $G$  synthesizes the UAEs  $\{(\tilde{x}_g, y_g)\}$  based on the perturbation and the specified class  $y_g$ . In G-D GAN, the discriminator  $D$  aims to adversarially distinguish the UAEs and the unobserved natural examples  $\{(x_l, y_l)\}$  generated by  $G$  from the true natural examples  $\{(x_l, y_l)\}$  with loss  $\mathcal{L}_{gan}^{G,D}$ , while in C-D GAN,  $D$  aims to adversarially distinguish the pseudo labeled examples  $\{(x_c, y_c)\}$  generated by the target classifier  $C$  from  $\{(x_l, y_l)\}$  with loss  $\mathcal{L}_{gan}^{C,D}$ . The extended AT is conducted between  $A$  and  $C$  with the adversarial loss  $\mathcal{L}_{adv}^{C,A}$  plus the supervised loss  $\mathcal{L}_{sup}^C$ .

lead to a suboptimal  $D$  [26], [27], and consequently weaken the ability of the G-D GAN to accurately align  $P_G(x, y)$  with  $P(x, y)$ . To alleviate this issue, we introduce another conditional GAN, called C-D GAN, which together with the G-D GAN constitutes the G-C-D GAN. The C-D GAN consists of the target classifier  $C$  and the discriminator  $D$ , where  $C$  aims at predicting the label  $y_c$  for unlabeled examples  $\{x_c \sim P(x)\}$  to build pseudo-labeled examples  $\{(x_c, y_c)\}$  that can fool  $D$ , while  $D$  tries to distinguish  $\{(x_c, y_c)\}$  from true examples  $\{(x_l, y_l)\}$ . The adversarial game between  $C$  and  $D$  improves the ability of  $D$  to identify whether a label matches an example  $x$ . As  $D$ 's role in C-D GAN is consistent with its role in G-D GAN,  $D$  strengthened by C-D GAN will ultimately help  $G$  capture the true data distribution  $P(x, y)$  more accurately.

At last, to realize the **comprehensive adversarial robustness** of the target classifier  $C$ , we want to align the  $P_G(x, y)$  with the distribution  $P_C(x, y)$  learned by  $C$ , which equivalently improves the robust generalizability of  $C$  on UAEs. For this purpose, we conduct AT between the attacker  $A$  and  $C$ , with an adversarial loss  $\mathcal{L}_{adv}^{A,C}$  over the generated UAEs. At the same time, to simultaneously improve the **standard generalizability** of  $C$  on natural examples, we further enforce the distribution  $P_C(x, y)$  to be aligned with the true data distribution  $P(x, y)$ , by extending the AT with minimization of the supervised loss  $\mathcal{L}_{sup}^C$  of  $C$  over the labeled data  $\{(x_l, y_l)\}$ . The overall logic of PUAT can be summarized as follows:

- (1) For the imperceptibility of UAEs,  $P_G(x, y)$  is aligned with the true data distribution  $P(x, y)$ , denoted by  $P_G(x, y) = P(x, y)$ , via the G-C-D GAN.
- (2) The harmfulness of UAEs is offered by the maximization of  $\mathcal{L}_{adv}^{A,C}$  during the AT.
- (3) The adversarial robustness is offered by  $P_C(x, y) = P_G(x, y)$ , via the inner minimization of  $\mathcal{L}_{adv}^{A,C}$  of the AT between  $A$  and  $C$ .
- (4) The standard generalizability is offered by  $P_C(x, y) = P(x, y)$ , via the minimization of  $\mathcal{L}_{sup}^C$ .

It is noteworthy that traditional AT methods only realize (3) and (4), which causes  $P_C(x, y)$  to be a mix of  $P_G(x, y)$  and  $P(x, y)$  and consequently incurs a tradeoff between ad-

versarial robustness and standard generalizability. In sharp contrast with the traditional methods, PUAT eliminates such tradeoff because (1) ( $P_G(x, y) = P(x, y)$ ), together with (3) and (4), results in the equivalence between adversarial robustness ( $P_C(x, y) = P_G(x, y)$ ) and standard generalizability ( $P_C(x, y) = P(x, y)$ ), i.e.,  $P_C(x, y) = P_G(x, y) = P(x, y)$ .

### 3.2 UAE Generation

Our idea to generate a UAE  $(\tilde{x}_g, y_g)$  is to perturb a generated natural example. Let  $P(y)$  be the label distribution and  $P_\epsilon(z)$  be a standard normal distribution. At first, we sample a label  $y_g \sim P(y)$ , and a seed noise  $z \sim P_\epsilon(z)$ . Then we invoke  $G$  to generate an example  $(x_g, y_g) \sim P_G(x, y)$ , where

$$x_g = G(z, y_g). \quad (2)$$

Note that since the label distribution  $P(y)$  is unknown, we use the labels appearing in the labeled dataset  $\mathcal{D}_l = \{(x_l, y_l) \sim P(x, y)\}$  to approximate it. In particular, the label  $y_l$  of each example in  $\mathcal{D}_l$  will serve as a  $y_g$  once.

To generate the UAE corresponding to  $(x_g, y_g)$ , we further feed  $(z, y_g)$  into the attacker  $A$  to produce the perturbation,

$$z_a = A(z, y_g). \quad (3)$$

Next,  $z_a$  together with  $y_g$  is fed into the generator  $G$  to produce perturbed data

$$\tilde{x}_g = G(z_a, y_g). \quad (4)$$

Finally,  $\tilde{x}_g$  and  $y_g$  together form a labeled UAE  $(\tilde{x}_g, y_g)$ .

It is noteworthy that that  $(x_g, y_g)$  can be regarded as an unobserved natural example if  $P_G(x, y)$  is aligned with the true data distribution  $P(x, y)$ . For each  $(x_g, y_g)$ , we will generate a corresponding UAE  $(\tilde{x}_g, y_g)$ , which is actually the perturbed  $(x_g, y_g)$  as they are generated based on the same  $(z, y_g)$  with the only difference that whether  $z$  or its perturbed version  $z_a = A(z, y_g)$  is fed into  $G$ . At the same time, as we will see later, during the AT between  $A$  and  $C$ ,  $A$  will be adjusted to ensure  $(\tilde{x}_g, y_g)$  be an adversarial example that is able to attack the classifier  $C$ , i.e.,  $C(\tilde{x}_g) \neq$

$y_g$ . Therefore, the UAEs  $\{(\tilde{x}_g, y_g)\}$  are a subset of  $\{(x_g, y_g)\}$  such that  $(\tilde{x}_g, y_g) \sim P_G(x, y|C(x) \neq y)$ , and essentially,  $A$  plays the role of finding out  $\{(\tilde{x}_g, y_g)\}$  from  $\{(x_g, y_g)\}$ .

### 3.3 Distribution Alignment for Imperceptibility

As mentioned before, the imperceptibility of UAEs results from the alignment of the distribution  $P_G(x, y)$  with the true data distribution  $P(x, y)$ , which is realized through the cooperation of G-D GAN and C-D GAN. Let  $\mathcal{D}_l = \{(x_l, y_l) \sim P(x, y)\}$  be a labeled natural dataset, where  $y_l = o(x_l)$ . Then the optimization objective of G-D GAN is defined as

$$\min_G \max_D \mathcal{L}_{gan}^{G,D} = \mathcal{L}_D + \mathcal{L}_G, \quad (5)$$

where

$$\begin{aligned} \mathcal{L}_D &= \mathbb{E}_{(x_l, y_l) \sim P(x, y)} \log D(x_l, y_l) \\ &= \frac{1}{|\mathcal{D}_l|} \sum_{(x_l, y_l) \in \mathcal{D}_l} \log D(x_l, y_l) \end{aligned} \quad (6)$$

and

$$\begin{aligned} \mathcal{L}_G &= \mathbb{E}_{(x_g, y_g) \sim P_G(x, y)} \log(1 - D(x_g, y_g)) \\ &= \frac{1}{|\mathcal{D}_l|} \sum_{(x_l, y_l) \in \mathcal{D}_l} \log\left(1 - D(G(z, y_l), y_l)\right). \end{aligned} \quad (7)$$

In Equation (7), the label  $y_l$  of each example  $(x_l, y_l) \in \mathcal{D}_l$  serves as  $y_g \sim P(y)$ . For each  $y_l$ , we first sample a noise  $z \sim P_\epsilon(z)$  and then invoke  $G(z, y_l)$  to generate  $x_g$ , which together with  $y_l$  forms a data-label pair  $(x_g, y_g)$ .

In G-D GAN, the generation of a data-label pair  $(x_g, y_g)$  can be understood as the procedure of first drawing  $y_g \sim P(y)$  and then drawing  $x_g|y_g \sim P_G(x|y)$ , where  $P_G(x|y)$  is the conditional distribution characterized by  $G$ . Therefore,  $(x_g, y_g) \sim P_G(x, y) = P(y)P_G(x|y)$ . As  $y_g$  is drawn from the true label distribution  $P(y)$ , to adversarially distinguish  $(x_g, y_g)$  from true examples, what  $D$  should do is to identify whether  $x_g|y_g$  is true. There is one of two reasons causing a false  $x_g|y_g$ . One is  $x_g$  is false, which asks  $D$  to identify whether  $x_g \sim P(x)$ . The other is although  $x_g$  is true, it does not belong to class  $y_g$ , which asks  $D$  to identify whether  $y_g|x_g \sim P(y|x)$ . However, as we have mentioned before, these two tasks conflict with each other for  $D$ , which leads to a suboptimal  $D$  and consequently weakens  $G$ . To alleviate this issue, we introduce C-D GAN and use an unlabeled natural dataset  $\mathcal{D}_c = \{x_c \sim P(x)\}$  to train it with the following optimization objective:

$$\min_C \max_D \mathcal{L}_{gan}^{C,D} = \mathcal{L}_D + \mathcal{L}_C, \quad (8)$$

where

$$\begin{aligned} \mathcal{L}_C &= \mathbb{E}_{(x_c, y_c) \sim P_C(x, y)} \log(1 - D(x_c, y_c)) \\ &= \frac{1}{|\mathcal{D}_c|} \sum_{x_c \in \mathcal{D}_c} \log(1 - D(x_c, y_c = C(x_c))). \end{aligned} \quad (9)$$

To calculate  $\mathcal{L}_C$ , for each  $x_c \in \mathcal{D}_c$ , we invoke the target classifier  $C$  to label it with the prediction  $y_c = C(x_c)$ , which generates a data-label pair  $(x_c, y_c)$ . This is equivalent to the procedure of first drawing  $x_c \sim P(x)$  and then drawing  $y_c|x_c \sim P_C(y|x)$ . Therefore  $(x_c, y_c) \sim P_C(x, y) = P(x)P_C(y|x)$ . C-D GAN offers two benefits to  $D$ . The first

is in C-D GAN,  $C$  provides the adversarial signal  $y_c|x_c$  to help  $D$  learn  $P(y|x)$ , which ultimately promotes  $D$ 's performance in G-D GAN for a better  $G$ . The second is in both C-D GAN and G-D GAN,  $D$  plays the same role of distinguishing the generated examples ( $\{(x_g, y_g)\}$  or  $\{(x_c, y_c)\}$ ) from true ones ( $\{(x_l, y_l)\}$ ), which eliminates the conflict optimization of  $D$  in traditional conditional GAN.

We refer to the combination of G-D GAN and C-D GAN as G-C-D GAN. By combining Equations (5) and (8), we obtain the following optimization objective for G-C-D GAN:

$$\min_{C,G} \max_D \mathcal{L}_{gan}^{G,C,D} = \mathcal{L}_D + \frac{1}{2} \mathcal{L}_G + \frac{1}{2} \mathcal{L}_C. \quad (10)$$

### 3.4 Extended Adversarial Training

Since the harmfulness of the generated UAEs is caused by the attacker  $A$ , we conduct the AT between  $A$  and the target classifier  $C$ . Meanwhile, to improve both the adversarial robustness and standard generalizability, we extend the AT defined in Equation (1) by incorporating the supervised loss of  $C$ , which leads to the following min-max game:

$$\min_C \max_A [\mathcal{L}_{sup}^C + \lambda \mathcal{L}_{adv}^{C,A}], \quad (11)$$

where  $\lambda$  is a non-negative constant controlling the weight of adversarial robustness and the standard generalizability. The supervised loss of the target classifier  $C$  is defined as

$$\begin{aligned} \mathcal{L}_{sup}^C &= \mathbb{E}_{(x, y) \sim P(x, y)} [-\log P_C(y|x)] \\ &= \frac{1}{|\mathcal{D}_l|} \sum_{(x_l, y_l) \in \mathcal{D}_l} [-\log P_C(y_l|x_l)]. \end{aligned} \quad (12)$$

where the conditional probability  $P_C(y|x)$  is the output of  $C$ . The adversarial loss is defined as

$$\begin{aligned} \mathcal{L}_{adv}^{C,A} &= \mathbb{E}_{(x, y) \sim P_G(x, y)} [-\log P_C(y|\tilde{x})] \\ &= \frac{1}{|\mathcal{A}|} \sum_{(\tilde{x}, y) \in \mathcal{A}} [-\log P_C(y|\tilde{x})], \end{aligned} \quad (13)$$

where  $\mathcal{A}$  is the generated UAE set. Note that for each  $(x, y) \sim P_G(x, y)$ , we generate its corresponding UAE  $(\tilde{x}, y)$  by invoking Equations (3) and (4) (see Section 3.2).

In Equation (11), the inner maximization of  $\mathcal{L}_{adv}^{C,A}$  enforces  $A$  to be adjusted so that a generated UAE  $(\tilde{x}_g, y_g)$  is harmful enough, i.e.,  $C(\tilde{x}_g) \neq y_g$ , which causes the UAE generation module (consisting of  $A$  and  $G$ ) to converge to the underlying UAE distribution  $P_G(x, y|C(x) \neq y)$  which maximizes the adversarial loss. The outer minimization realizes the alignment  $P_C(x, y) = P_G(x, y|C(x) \neq y)$  by adjusting  $C$ , which results in  $C$ 's robust generalizability over UAEs (i.e. the adversarial robustness). As proved later, the KL-divergence of  $P_C(x, y)$  and  $P_G(x, y|C(x) \neq y)$  is the upper bound of the KL-divergence of  $P_C(x, y)$  and  $P_G(x, y)$ . Therefore, the minimization of  $\mathcal{L}_{adv}^{C,A}$  will approximately lead to  $P_C(x, y) = P_G(x, y)$ . At the same time, one can note that the minimization of  $\mathcal{L}_{sup}^C$  will be achieved when  $P_C(x, y) = P(x, y)$ , which offers  $C$  the standard generalizability on natural examples. Later we will prove that with the help of the G-C-D GAN (Equation(10)), the extended AT defined by Equation(11) will achieve the optimal solution at  $P_C(x, y) = P_G(x, y) = P(x, y)$ , which means the adversarial robustness and the standard generalizability are satisfied simultaneously.

**Algorithm 1** Training Algorithm of PUAT

---

**Input:** Datasets  $\mathcal{D}_l$  and  $\mathcal{D}_u$ ;  
**Output:** Well-trained target classifier  $C$ ;

- 1: Random initialize  $A$ ,  $C$ ,  $G$ , and  $D$ ;
- 2: **for**  $T$  epochs **do**
- 3: Generate UAE set  $\mathcal{A}$  using Equations (3) and (4).
- 4: Generate examples  $\{(x_g, y_g) \sim P_G(x, y)\}$  based on  $\mathcal{D}_l$  w.r.t. Equation (7).
- 5: Generate examples  $\{(x_c, y_c) \sim P_C(x, y)\}$  based on  $\mathcal{D}_u$  w.r.t. Equation (9).
- 6: Update  $D$  by **ascending** stochastic gradient  $\nabla_D(\mathcal{L}_{gan}^{C,D} + \mathcal{L}_{gan}^{G,D})$ ;
- 7: Update  $A$  by **ascending** stochastic gradient  $\nabla_A(\mathcal{L}_{adv}^{C,A})$ ;
- 8: Update  $C$  by **descending** stochastic gradient  $\nabla_C(\mathcal{L}_{gan}^{C,D} + \mathcal{L}_{supC}^C + \lambda\mathcal{L}_{adv}^{C,A})$ ;
- 9: Update  $G$  by **descending** stochastic gradient  $\nabla_G(\mathcal{L}_{gan}^{G,D})$ ;
- 10: **end for**

---

### 3.5 Joint Training

By combining Equations (10) and (11), we can obtain the following overall optimization objective for joint learning of  $A$ ,  $G$ ,  $C$  and  $D$ :

$$\min_{C,G} \max_{A,D} [\mathcal{L}_{gan}^{G,C,D} + \mathcal{L}_{sup}^C + \lambda\mathcal{L}_{adv}^{C,A}]. \quad (14)$$

Basically, Equation (14) integrates the adversarial generation of UAEs and the AT over UAEs within a unified min-max game. Algorithm 1 gives the sketch of the joint training, where the Lines 6 and 7 solve the inner maximization with stochastic gradient ascent, while the Lines 8 and 9 solve the outer minimization with stochastic gradient descent.

## 4 THEORETICAL JUSTIFICATION

In this section, we theoretically justify PUAT's ability to simultaneously improve adversarial robustness and standard generalizability of the target classifier without compromising either of them. Recall that PUAT offers the adversarial robustness by  $P_C(x, y) = P_G(x, y)$ , while the standard generalizability by  $P_C(x, y) = P(x, y)$ . As Equation (14) defines a unified framework integrating the UAE generation with the AT against UAEs, proving PUAT's ability to eliminate the tradeoff is equivalent to proving that the optimal solution of Equation (14) will be achieved at  $P_C(x, y) = P_G(x, y) = P(x, y)$ , which means the adversarial robustness and the standard generalizability agree with each other under the framework of Equation (14). For the brevity of later derivations, in the following text  $P(x, y)$ ,  $P_G(x, y)$  and  $P_C(x, y)$  will be abbreviated to  $P$ ,  $P_G$  and  $P_C$ , respectively, when the context is unambiguous. We first give the equilibrium of the G-C-D GAN by the following lemma:

**Lemma 1.** *The optimal solution ( $G^*$ ,  $C^*$ ,  $D^*$ ) of  $\min_{C,G} \max_D \mathcal{L}_{gan}^{G,C,D}$  (Equation (10)) is achieved at  $p = \frac{1}{2}(P_G + P_C)$ .*

*Proof.* Let  $P_{GC} = \frac{1}{2}(P_G + P_C)$ . According to Equations (6), (7), (9) and (10), it is easy to see

$$\mathcal{L}_{gan}^{G,C,D} = \iint P \log D dx dy + \iint P_{GC} \log(1 - D) dx dy. \quad (15)$$

Fixing  $G$  and  $C$ , the optimal discriminator [28]

$$D^* = \operatorname{argmax}_D \mathcal{L}_{gan}^{G,C,D} = \frac{P}{P + P_{GC}}. \quad (16)$$

Plugging  $D^*$  in Equation (15) and by some tedious derivations, we can get

$$\begin{aligned} \mathcal{L}_{gan}^{G,C,D^*} &= \iint \left[ P \log \left( \frac{P}{\frac{1}{2}(P + P_{GC})} \right) \right. \\ &\quad \left. + P_{GC} \log \left( \frac{P_{GC}}{\frac{1}{2}(P + P_{GC})} \right) \right] dx dy - 2 \log 2 \\ &= \text{JS}(P \parallel P_{GC}) - 2 \log 2, \end{aligned} \quad (17)$$

where JS is Jensen-Shannon divergence. Since  $\text{JS}(p \parallel P_{GC}) \geq 0$ ,  $G^*$  and  $C^*$  are achieved at  $\text{JS}(P \parallel P_{GC}) = 0$ , which leads to  $P = P_{GC} = \frac{1}{2}(P_G + P_C)$ .  $\square$

Now we show that  $\min_C \mathcal{L}_{sup}^C$  and  $\min_C \max_A \mathcal{L}_{adv}^{C,A}$  are two consistent optimization problems with the same optimal solution  $C$  at which  $P_C(x, y) = P_G(x, y) = P(x, y)$ .

**Theorem 1.** *In Equation (11),  $\min_C \mathcal{L}_{sup}^C$  and  $\min_C \max_A \mathcal{L}_{adv}^{C,A}$  can be achieved at the same optimal  $C$  subjected to  $P_C(x, y) = P_G(x, y) = P(x, y)$ .*

*Proof.* (1) By the definition of  $\mathcal{L}_{sup}^C$  (Equation (12)), the optimal  $C$  for  $\min_C \mathcal{L}_{sup}^C$  is

$$\begin{aligned} &\operatorname{argmin}_C \mathcal{L}_{sup}^C \\ &= \operatorname{argmin}_C \iint \left[ -P(x, y) \log(P_C(y|x)P(x)) + \right. \\ &\quad \left. P(x, y) \log P(x, y) \right] dx dy \\ &= \operatorname{argmin}_C \iint P(x, y) \log \frac{P(x, y)}{P_C(x, y)} dx dy \\ &= \operatorname{argmin}_C \text{KL}(P(x, y) \parallel P_C(x, y)), \end{aligned}$$

where KL is Kullback–Leibler divergence, the first equality holds because  $P(x)$  and  $P(x, y)$  are independent of  $C$  without changing the monotonicity of  $\mathcal{L}_{sup}^C$ , and the second equality holds because  $P_C(x, y) = P(x)P_C(y|x)$ . Therefore,  $\min_C \mathcal{L}_{sup}^C$  is achieved at  $P_C(x, y) = P(x, y)$ . Note that when  $C$  is adjusted with respect to  $P_C(x, y) = P(x, y)$ , G-C-D GAN (Equation (10)) will synchronically adjust  $G$  with respect to  $P_G(x, y) = P(x, y)$ , to keep the equilibrium of  $G$ ,  $C$  and  $D$  (Lemma 1). We hence can safely substitute  $P(x, y)$  for  $P_C(x, y)$  in  $P(x, y) = \frac{1}{2}(P_G(x, y) + P_C(x, y))$  (Lemma 1), which follows that

$$P_C(x, y) = P_G(x, y) = P(x, y).$$

(2) According to Equation (13), we have

$$\operatorname{argmin}_C \max_A \mathcal{L}_{adv}^{C,A} \quad (18)$$

$$= \operatorname{argmin}_C \max_A \iint -P_G(x, y) \log P_C(y|\tilde{x}) dx dy \quad (19)$$

$$= \operatorname{argmin}_C \max_A \iint \left[ -P_G(x, y) \log P_C(\tilde{x}, y) \right. \\ \left. + P_G(x, y) \log P_G(x, y) \right] dx dy \quad (20)$$

$$= \operatorname{argmin}_C \max_A \iint P_G(x, y) \log \frac{P_G(x, y)}{P_C(\tilde{x}, y)} dx dy \quad (22)$$

$$= \operatorname{argmin}_C \max_A \text{KL}(P_G(x, y) \parallel P_C(\tilde{x}, y)). \quad (23)$$

Obviously,

$$\begin{aligned} & \max_A \iint P_G(x, y) \log \frac{P_G(x, y)}{P_C(\tilde{x}, y)} dx dy \\ & \geq \iint P_G(x, y) \log \frac{P_G(x, y)}{P_C(x, y)} dx dy \\ & = \text{KL}(P_G(x, y) \parallel P_C(x, y)), \end{aligned}$$

which indicates that  $\min_C \max_A \mathcal{L}_{adv}^{C,A}$  essentially minimizes the upper-bound of the KL-divergence of  $P_G(x, y)$  and  $P_C(x, y)$ .

Let  $P_{G|A}(x, y) = P_G(x, y | C(x) \neq y)$  be the UAE distribution. Noting that the UAEs  $\{(x, y) \sim P_{G|A}(x, y)\}$  maximize the adversarial loss  $\mathcal{L}_{adv}^{C,A}$  (Equation (13)), which are found out by  $A$ , we hence also have

$$\begin{aligned} & \operatorname{argmin}_C \max_A \mathcal{L}_{adv}^{C,A} \quad (24) \\ & = \operatorname{argmin}_C \iint -P_{G|A}(x, y) \log P_C(y|x) dx dy \quad (25) \\ & = \operatorname{argmin}_C \iint -P_{G|A}(x, y) \log P_C(x, y) dx dy \quad (26) \\ & = \operatorname{argmin}_C \iint \left[ -P_{G|A}(x, y) \log P_C(x, y) \right. \quad (27) \\ & \quad \left. + P_{G|A}(x, y) \log P_{G|A}(x, y) \right] dx dy \quad (28) \\ & = \operatorname{argmin}_C \iint P_{G|A}(x, y) \log \frac{P_{G|A}(x, y)}{P_C(x, y)} dx dy \quad (29) \\ & = \operatorname{argmin}_C \text{KL}(P_{G|A}(x, y) \parallel P_C(x, y)). \quad (30) \end{aligned}$$

Considering Equations (23) and (30), we can see that aligning  $P_{G|A}(x, y)$  with  $P_C(x, y)$  (i.e., minimizing  $\text{KL}(P_{G|A}(x, y) \parallel P_C(x, y))$ ) is equivalent to minimizing the upper-bound of  $\text{KL}(P_G(x, y) \parallel P_C(x, y))$ , which approximately leads to  $P_C(x, y) = P_G(x, y)$  and also results in

$$P_C(x, y) = P_G(x, y) = P(x, y).$$

(3) The part (1) and part (2) together tell us both  $\min_C \mathcal{L}_{sup}^C$  and  $\min_C \max_A \mathcal{L}_{adv}^{C,A}$  will lead to  $P_C(x, y) = P_G(x, y) = P(x, y)$ . Therefore, they are consistent optimization problems with the same optimal solution  $C$ .  $\square$

Theorem 1 together with Lemma 1 tells us that  $G$ ,  $C$  and  $D$  will reach their equilibrium when  $P_C(x, y) = P_G(x, y) = P(x, y)$ , which implies that the adversarial robustness ( $P_C(x, y) = P_G(x, y)$ ) and the standard generalizability ( $P_C(x, y) = P(x, y)$ ) can be simultaneously achieved by PUAT.

## 5 EXPERIMENTS

The goal of experiments is to answer the following research questions:

- **RQ1** How does PUAT perform as compared to the state-of-the-art baselines in terms of the standard generalizability and comprehensive adversarial robustness?
- **RQ2** Can PUAT provide comprehensive adversarial robustness against black-box attacks?
- **RQ3** How does the sensitivity of PUAT to the hyperparameter  $\lambda$  in Equation (14) show that the tradeoff between standard generalizability and adversarial robustness is eliminated by PUAT?
- **RQ4** How to visually show the superiority of PUAT?

TABLE 1  
Configuration of the datasets.

Datasets	unlabeled data	labeled data		
	training	training	validation	testing
CIFAR10	46,000	4,000	1,000	9,000
SVHN	72,257	1,000	250	25,782

TABLE 2  
Characteristics of the baseline methods and PUAT.

Methods	RAE	UAE	distribution alignment	using labeled data	using unlabeled data
Regular-training				✓	
TRADES [31]	✓			✓	
GAT [14]	✓			✓	
GPGD-AT [32]		✓		✓	
RST [33]	✓			✓	✓
PUAT		✓	✓	✓	✓

## 5.1 Experimental Setting

### 5.1.1 Datasets

We conduct the experiments on CIFAR10 [29] and SVHN [30], which are widely used benchmarks for evaluating adversarial training. CIFAR10 contains 60,000 images distributed across 10 classes, while SVHN is a set of 99,559 digit images. Each dataset is randomly divided into two parts, labeled data and unlabeled data, where unlabeled data are built by removing the labels of the images. The labeled data are further randomly divided into training set, validation set, and testing set. Table 1 shows the dataset configurations. We will repeat the random division of the dataset three times, and report the average results with standard deviation.

### 5.1.2 Baseline Methods

To verify the superiority of PUAT, we compare it with the following baseline methods, whose characteristics are summarized in Table 2.

- **Regular-training** Regular-training method trains the target classifier using natural data with cross-entropy loss, which plays the role of performance benchmark.
- **TRADES** [31] TRADES is an AT method based on RAEs that are generated by PGD based on labeled data, which can trade adversarial robustness off against standard generalizability by optimizing a regularized surrogate loss.
- **GAT** [14] GAT is an AT method based on RAEs that are generated by a GAN, where the generator produces explicitly norm-constrained adversarial perturbations for natural labeled examples with respect to the gradients of the target classifier loss.
- **GPGD-AT** [32] GPGD-AT is an AT method based on UAEs that are generated by GPGD [32]. To generate a UAE, GPGD first employs a conditional GAN to produce an unobserved natural labeled example, and then adds

TABLE 3  
Hyper-parameter setting of the attacking methods.

Attacks	Hyper-parameter setting
FGSM [8]	$\epsilon = 0.0031$ ; step size = 0.007.
PGD [9]	$\epsilon = 0.0031$ ; step size = 0.007; number of iterations = 10.
GPGD [32]	$\epsilon = 0.1$ on CIFAR10, 0.3 on SVHN; step size = 0.007; number of iterations = 10.
USong [16]	$\epsilon = 0.1$ on CIFAR10, 0.3 on SVHN; step size = 0.1, number of iterations = 200; $\lambda_1 = 100, \lambda_2 = 100$ .

adversarial perturbation to it based on the gradient of the target classifier loss incurred by it.

- **RST** [33] RST is also an AT method based on RAEs that are generated by PGD. Different from TRADES, RST first trains a classifier to predict labels for unlabeled data and then feeds these pseudo-labeled data together with labeled data into the sequel adversarial training algorithm.

Additionally, to verify the contribution of unlabeled data, we also compare PUAT with its variant **PUAT-L**, which does not use unlabeled data  $\mathcal{D}_c$  in Equation (9) but instead uses  $x_l$  in labeled data  $\mathcal{D}_l$  as  $x_c$  to compute  $\mathcal{L}_C$ .

### 5.1.3 Evaluation Protocol

We will use PUAT and the baseline methods to train the target classifier and compare their performances from the perspectives of the target classifier’s standard generalizability and adversarial robustness. The generalizability is evaluated in terms of the target classifier’s **natural accuracy** on testing natural examples, while the adversarial robustness is evaluated in terms of the target classifier’s **robust accuracy** on the testing adversarial examples which are generated by various attack methods. In particular, for the robustness against RAE, we choose FGSM [8] and PGD [9] to generate testing RAEs, which are the attacking methods widely adopted by the existing works. For the robustness against UAE, we choose GPGD [32] and USong [16] as the attacking methods, both of which are GAN-based methods and dedicated to the generation of UAEs. The hyper-parameters of the attacking methods are set to their optimal values, which are shown in Table 3. To evaluate the performance of PUAT and the baseline methods, we first invoke the attacking methods to generate testing AEs that can cause worst-case loss of the target classifier well trained by PUAT or a baseline method, and then check the classifier’s accuracy on those testing AEs.

To comprehensively evaluate the performance of PUAT and the baseline methods, we will investigate the robustness of the well-trained target classifier under two threat models, i.e., white-box attack and black-box attack. To examine a classifier’s robustness under white-box attacks, we first invoke the attacking methods to generate adversarial examples (RAEs or UAEs) that can cause worst-case loss of the target classifier trained by PUAT or a baseline method, and then check the classifier’s accuracy on those adversarial examples. To carry out the black-box attacks, each classifier trained by PUAT or a baseline method will also play as a

surrogate model of the classifiers trained by the other methods. To examine a classifier’s robustness under black-box attacks, we first invoke the attacking methods to conduct while-box attacks on its surrogate models, and then check its accuracy on the adversarial examples generated for the white-box attacks.

### 5.1.4 Hyper-parameter Setting and Architecture

The hyper-parameters are tuned on validation dataset. In particular, the  $\lambda$  in Equation 14 is set to 1. The perturbation constraint  $\epsilon$  in TRADES, GAT and RST is set to 0.031. The perturbation step size and the number of iterations in TRADES and RST are set to 0.007 and 10, respectively. The architecture of PUAT is shown in Table 4, where the generator  $G$ , discriminator  $D$ , and target classifier  $C$  are implemented with respect to those adopted in [26]. In the baseline methods, the architecture of the target classifiers is as the same as that of  $C$ .

## 5.2 Performance under White-box Attack (RQ1)

Tables 5 and 6 show the results under white-box attacks on CIFAR10 and SVHN, respectively, from which we can make the following observations:

- On both datasets, PUAT surpasses all baselines in robust accuracy under all assaults, with the exception of RST under PGD attack on CIFAR10, and achieves the highest natural accuracy, surpassing even regular-training. PUAT is the only AT approach that simultaneously increases standard generalizability and adversarial robustness against all attacks on both datasets, in contrast to baseline AT methods, which all produce at least one output that is subpar to regular-training. By aligning the AE distribution and natural data distribution, which results in a consistent generalization on AEs and natural data, we contend that this finding demonstrates PUAT’s capacity to eliminate the tradeoff between the standard generalizability and the adversarial robustness.
- We can see that, under the PGD attack, PUAT is superior to RST on SVHN but inferior to RST on CIFAR10. As a result, RST’s robustness against PGD attack is superior on datasets with dense labeled data, like CIFAR10, but inferior on datasets with sparse labeled data, like SVHN. This is because RST uses PGD to generate RAEs based on observed labeled examples, which makes it more robust against PGD attack on dense datasets. In other words, because of its distinctive generative model G-C-D GAN, PUAT can provide a stronger defense than baseline methods especially on sparse datasets.
- On both datasets, it is important to notice that PUAT beats nearly all defensive methods against RAE attacks (provided by FGSM and PGD) and UAE attacks (provided by GPGD and USong). The horizontal view, meanwhile, demonstrates that PUAT performs comparably to both sorts of attacks. These results show how effective PUAT is at providing comprehensive adversarial robustness against RAE and UAE attacks. We contend that the comprehensive adversarial robustness is made possible by our innovative notion to generalize the UAE concept to imperceptibly perturbed natural examples, whether observable or unobservable.

TABLE 4  
Model architecture of  $C$ ,  $D$ ,  $G$  and  $A$  of PUAT.

Classifier C	Discriminator D	Generator G	Attacker A
Input: $3 \times 32 \times 32$ image $x$	Input: $3 \times 32 \times 32$ image $x$ , label $y$	Input: noise $z$ , label $y$	Input: noise $z$ , label $y$
$3 \times 3$ conv, 128, lReLU, weight norm $3 \times 3$ conv, 128, lReLU, weight norm $3 \times 3$ conv, 128, lReLU, weight norm $2 \times 2$ max-pooling, 0.5 dropout	2-layer $3 \times 3$ residual block, 512, ReLU, spectral norm downsample $512 \times 16 \times 16$ 2-layer $3 \times 3$ residual block, 512, ReLU, spectral norm	MLP $8 \times 64 \times 16$ units reshape $512 \times 4 \times 4$ upsample $512 \times 8 \times 8$ 2-layer residual block, $3 \times 3$ conv, 512, ReLU, batch norm	MLP 256 + 256 units ReLU
$3 \times 3$ conv, 128, lReLU, weight norm $3 \times 3$ conv, 128, lReLU, weight norm $3 \times 3$ conv, 128, lReLU, weight norm $2 \times 2$ max-pooling, 0.5 dropout	downsample $512 \times 8 \times 8$ 2-layer $3 \times 3$ residual block, 512, ReLU, spectral norm	upsample $512 \times 16 \times 16$ 2-layer residual block, $3 \times 3$ conv, 512, ReLU, batch norm	
$3 \times 3$ conv, 512, lReLU, weight norm NIN, 256, lReLU, weight norm NIN, 128, lReLU, weight norm global pool	downsample $512 \times 4 \times 4$ 2-layer $3 \times 3$ residual block, 512, ReLU, spectral norm global pool	upsample $512 \times 32 \times 32$ 2-layer residual block, $3 \times 3$ conv, 512, ReLU, batch norm	
10-class softmax, weight norm	MLP 1 units, spectral norm	$1 \times 1$ conv, 3, tanh, batch norm	MLP 256 units, ReLU

TABLE 5  
Performance under white-box attacks on **CIFAR10**.

Methods	Natural Accuracy	Robust Accuracy			
		RAE Attack		UAE Attack	
		FGSM	PGD	GPGD	USong
Regular-training	$70.52 \pm 1.62$	$29.43 \pm 1.10$	$24.97 \pm 1.08$	$28.21 \pm 3.83$	$44.83 \pm 5.08$
TRADES	$65.59 \pm 2.25$	$57.09 \pm 0.93$	$55.65 \pm 0.96$	$19.71 \pm 1.24$	$37.14 \pm 2.12$
GAT	$69.68 \pm 2.00$	$50.57 \pm 3.14$	$44.94 \pm 3.09$	$27.01 \pm 4.54$	$45.59 \pm 4.84$
GPGD-AT	$72.62 \pm 0.77$	$29.06 \pm 1.03$	$24.52 \pm 1.22$	$37.55 \pm 2.66$	$49.32 \pm 0.75$
RST	$73.89 \pm 0.22$	$65.34 \pm 0.82$	<b><math>63.73 \pm 0.81</math></b>	$27.47 \pm 0.99$	$56.42 \pm 2.23$
PUAT-L	$76.96 \pm 0.89$	$49.64 \pm 2.11$	$43.27 \pm 1.97$	$55.18 \pm 1.19$	$63.83 \pm 2.43$
PUAT	<b><math>83.47 \pm 0.60</math></b>	<b><math>67.51 \pm 0.10</math></b>	$58.76 \pm 0.29$	<b><math>59.49 \pm 2.14</math></b>	<b><math>81.65 \pm 0.51</math></b>

TABLE 6  
Performance under white-box attacks on **SVHN**

Methods	Natural Accuracy	Robust Accuracy			
		RAE Attack		UAE Attack	
		FGSM	PGD	GPGD	USong
Regular-training	$86.12 \pm 0.43$	$52.16 \pm 2.25$	$50.51 \pm 2.33$	$58.77 \pm 2.48$	$80.42 \pm 2.14$
TRADES	$80.86 \pm 1.96$	$57.15 \pm 2.90$	$56.51 \pm 2.90$	$27.56 \pm 7.75$	$62.79 \pm 3.14$
GAT	$81.01 \pm 2.35$	$55.52 \pm 0.81$	$53.50 \pm 0.77$	$45.72 \pm 4.85$	$64.56 \pm 3.64$
GPGD-AT	$77.99 \pm 1.88$	$44.16 \pm 0.11$	$42.23 \pm 0.29$	$49.42 \pm 0.75$	$58.34 \pm 1.69$
RST	$87.59 \pm 0.62$	$62.69 \pm 2.84$	$62.04 \pm 2.85$	$44.78 \pm 4.70$	$79.19 \pm 0.89$
PUAT-L	$87.64 \pm 0.68$	$59.17 \pm 1.32$	$56.75 \pm 1.24$	$70.41 \pm 0.90$	$88.14 \pm 2.11$
PUAT	<b><math>90.35 \pm 0.33</math></b>	<b><math>67.08 \pm 0.58</math></b>	<b><math>64.33 \pm 0.46</math></b>	<b><math>77.39 \pm 1.59</math></b>	<b><math>95.52 \pm 0.80</math></b>

- The RAE-based AT methods TRADES and GAT enhance robust accuracy under RAE attacks at the expense of natural accuracy when compared to regular-training. This demonstrates distribution-shift between natural data and AEs will result from traditional AT methods that put norm-constraint on perturbations, which leads to a trade-off between the standard generalizability and the adversarial robustness. They are also less accurate under UAE attacks than regular-training, which shows that they are unable to provide adversarial robustness against UAEs.
- PUAT absolutely defeats GPGD-AT under UAE attacks on both datasets, despite the fact that it is also an AT method based on UAE. This is mostly due to the introduction of the C-D GAN and the unlabeled data for improved

distribution alignment in PUAT. Target classifier  $C$  particularly aids the discriminator  $D$  in comprehending the distribution  $P(y|x)$  via C-D GAN, and finally via G-D GAN aids the generator  $G$  in accurately capturing the natural data distribution. In contrast, GPGD-AT only uses one conditional GAN, which prevents it from properly aligning the UAE distribution with the natural data distribution. Meanwhile, it is noteworthy that GPGD-AT, which relies on labeled data, performs even worse under UAE attacks on the sparse dataset SVHN than regular-training.

- When it comes to natural accuracy and robust accuracy against RAE attacks, RST is the second-best method after PUAT. When compared to other RAE-based methods, RST’s generalization over natural examples and RAEs is superior because it introduces unlabeled examples to help it achieve a tighter upper-bound of the tradeoff. This method also mitigates the tradeoff between standard generalizability and adversarial robustness. The tradeoff hasn’t gone away, though, and we can see that because of RAE-based AT’s fundamental limitations, RST could hardly defend against UAE attacks on either dataset.
- Finally, we observe that PUAT-L performs significantly worse than PUAT, which validates the contribution of unlabeled examples to PUAT. As previously mentioned, PUAT trains the target classifier to provide pseudo labels for unlabeled examples. This aids the G-C-D GAN in accurately understanding  $P(y|x)$  and, in turn, enables the target classifier to generalize consistently over aligned distributions of natural data and AEs. However, due to G-C-D GAN’s capability to align the UAE distribution with natural data distribution, PUAT-L is still superior to the other baseline methods in natural accuracy and robust-accuracy under UAE attacks.

### 5.3 Performance under Black-box Attack (RQ2)

As previously mentioned, to conduct the black-box attacks, we first invoke an attacking method to attack the surrogate model pre-trained by a defensive method to generate AEs, and then use these AEs to attack the target classifiers trained by other defensive methods. Since PGD and GPGD are the most successful white-box attacking methods in our experiments, we select them as the black-box attackers. Tables 7 and 8 display the results for CIFAR10, whereas Tables 9 and 10 display the results for SVHN.

Let’s start by focusing the last row of each table. As we can see, PUAT achieves the best robust accuracy in each scenario, demonstrating that it is more powerful than all baseline methods at resisting black-box attacks. Considering PUAT’s excellent performance in defending against white-box attacks, we are not surprised by this outcome. The most intriguing part of each table is the last column, which shows how well baseline approaches fight against AEs produced by attacking the surrogate model trained by PUAT. We can see that in the majority of cases, the black-box attacks based on the surrogate model trained by PUAT result in better robust accuracy for baseline methods than those based on surrogate models trained by other baseline methods, demonstrating the lower threat of the surrogate model trained by PUAT. As a result, this finding shows that PUAT is not only the most resilient against black-box attacks but also does not support them.

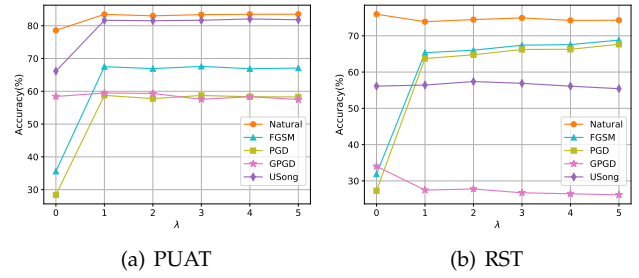


Fig. 3. Elimination of the tradeoff between standard generalizability and adversarial robustness.

### 5.4 Elimination of The Tradeoff (RQ3)

Now we examine PUAT’s performance throughout a range of values of the factor  $\lambda$ , which regularizes the weights of standard generalization and adversarial robustness in Equation (14), to see if it can eliminate the tradeoff between them. Figure 3(a) shows the curves of PUAT’s natural accuracy and robust accuracies under different attacks on CIFAR10. As we can see, all of the curves first rise as we increase  $\lambda$  from 0 to 1, and then roughly stabilize, which demonstrates that when  $\lambda$  is bigger than 0, it has no regulatory influence on the training of PUAT. In other words, PUAT can consistently optimize both adversarial robustness and standard generalization without having to make a tradeoff between them. This is due to PUAT’s ability to reconcile the robust generalization on AEs and the standard generalization on natural data by aligning the AE generator distribution  $P_G(x, y)$ , the target classifier distribution  $P_C(x, y)$  and the natural data distribution  $P(x, y)$ , as previously proved in Section 4.

Similarly, RST also has a balance factor  $\lambda$  to weight the importance of adversarial loss during its training. In contrast to PUAT, the robust accuracy of RST on RAEs (by FGSM and PGD) is gradually increasing as  $\lambda$  increases, but its natural accuracy decreases in parallel, as shown in Figure 3(b). This indicates that there is a tradeoff between the adversarial robustness and standard generalizability due to their conflicting optimization objectives in RST. At the same time, one can note that since GPGD and USong generate UAEs from the natural data distribution, the decrease in the standard generalization of RST on natural data naturally leads to a concomitant decrease in its adversarial robustness against UAEs. In sharp contrast, in Figure 3(a), PUAT’s robust accuracies on GPGD and USong exhibit the same pattern as its robust accuracies on PGD and FGSM, demonstrating once more that PUAT is capable of providing consistent adversarial robustness against both UAE and RAE since PUAT regards RAE as a special UAE.

### 5.5 Visual Study (RQ4)

Now, we visually demonstrate PUAT’s capability to align the natural data distribution  $P(x, y)$ , the distribution  $P_G(x, y)$  learned by the generator, and the distribution  $P_C(x, y)$  learned by target classifier. For this purpose, on each testing set, we first sample three different class labels  $y_1, y_2$  and  $y_3$  from  $P(y)$ , with  $y_1 = \text{“airplane”}$ ,  $y_2 = \text{“automobile”}$ ,  $y_3 = \text{“bird”}$  on CIFAR10 and  $y_1 = \text{“0”}$ ,

TABLE 7  
Adversarial robustness against black-box attacks of PGD on CIFAR10

Target Models	Surrogate Models trained by						
	Regular-training	TRADES	GAT	GPGD-AT	RST	PUAT-L	PUAT
Regular-training	—	33.03 ± 1.20	31.50 ± 1.18	31.50 ± 1.31	32.58 ± 1.28	31.89 ± 1.32	<b>33.23 ± 1.29</b>
TRADES	58.78 ± 0.99	—	58.57 ± 0.96	58.77 ± 0.93	57.82 ± 0.91	58.58 ± 0.89	<b>58.84 ± 0.89</b>
GAT	55.06 ± 3.07	55.95 ± 2.83	—	55.50 ± 2.89	55.63 ± 3.01	55.06 ± 2.93	<b>56.40 ± 3.03</b>
GPGD-AT	36.43 ± 2.94	38.24 ± 2.63	37.04 ± 2.56	—	37.94 ± 2.66	36.69 ± 2.58	<b>38.39 ± 2.63</b>
RST	66.93 ± 0.76	65.97 ± 0.80	66.66 ± 0.85	66.94 ± 0.78	—	66.79 ± 0.72	66.89 ± 0.77
PUAT-L	52.23 ± 2.27	52.89 ± 2.04	51.97 ± 2.27	51.88 ± 2.04	52.60 ± 2.03	—	<b>53.09 ± 2.10</b>
PUAT	<b>74.55 ± 0.38</b>	<b>74.55 ± 0.26</b>	<b>73.59 ± 0.40</b>	<b>74.17 ± 0.50</b>	<b>74.03 ± 0.25</b>	<b>73.37 ± 0.49</b>	—

TABLE 8  
Adversarial robustness against black-box attacks of GPGD on CIFAR10

Target Models	Black-box from Surrogate Models trained by						
	Regular-training	TRADES	GAT	GPGD-AT	RST	PUAT-L	PUAT
Regular-training	—	49.77 ± 1.12	46.16 ± 1.34	50.49 ± 3.15	40.09 ± 1.78	59.07 ± 0.89	<b>63.36 ± 1.50</b>
TRADES	57.61 ± 1.30	—	55.04 ± 0.76	58.21 ± 0.36	37.41 ± 1.05	62.11 ± 1.46	<b>64.39 ± 1.91</b>
GAT	49.40 ± 2.49	46.21 ± 1.15	—	54.12 ± 3.53	42.83 ± 1.04	61.29 ± 1.26	<b>64.07 ± 1.31</b>
GPGD-AT	53.81 ± 1.00	54.56 ± 0.36	56.11 ± 1.65	—	49.77 ± 0.59	63.46 ± 0.25	<b>67.38 ± 0.75</b>
RST	61.88 ± 1.87	47.96 ± 1.41	62.91 ± 0.49	65.60 ± 1.67	—	68.70 ± 0.60	<b>71.31 ± 1.11</b>
PUAT-L	54.91 ± 1.09	55.20 ± 1.09	57.72 ± 0.63	57.23 ± 2.26	47.54 ± 0.98	—	<b>67.93 ± 1.17</b>
PUAT	<b>78.09 ± 0.22</b>	<b>77.84 ± 0.54</b>	<b>78.40 ± 0.61</b>	<b>77.80 ± 1.59</b>	<b>71.60 ± 0.46</b>	<b>79.09 ± 0.50</b>	—

TABLE 9  
Adversarial robustness against black-box attacks of PGD on SVHN

Target Models	Black-box from Surrogate Models trained by						
	Regular-training	TRADES	GAT	GPGD-AT	RST	PUAT-L	PUAT
Regular-training	—	53.37 ± 2.19	53.08 ± 2.28	53.64 ± 2.25	53.35 ± 2.22	53.22 ± 2.18	<b>54.05 ± 2.07</b>
TRADES	58.04 ± 2.71	—	57.96 ± 2.71	58.33 ± 2.69	57.69 ± 2.71	58.03 ± 2.69	<b>58.39 ± 2.63</b>
GAT	57.24 ± 1.01	57.4 ± 1.12	—	58.21 ± 1.04	57.70 ± 1.08	57.41 ± 0.98	<b>58.34 ± 1.11</b>
GPGD-AT	45.87 ± 0.43	46.27 ± 0.47	46.16 ± 0.41	—	46.31 ± 0.48	46.10 ± 0.38	<b>46.71 ± 0.34</b>
RST	63.09 ± 2.79	62.87 ± 2.82	63.11 ± 2.80	63.39 ± 2.83	—	63.14 ± 2.77	63.30 ± 2.74
PUAT-L	60.03 ± 1.45	60.35 ± 1.37	60.06 ± 1.29	60.93 ± 1.22	60.39 ± 1.30	—	60.89 ± 1.26
PUAT	<b>69.13 ± 0.98</b>	<b>69.03 ± 0.90</b>	<b>68.89 ± 0.84</b>	<b>69.45 ± 0.99</b>	<b>68.88 ± 1.04</b>	<b>68.91 ± 0.93</b>	—

TABLE 10  
Adversarial robustness against black-box attacks of GPGD on SVHN

Target Models	Black-box from Surrogate Models trained by						
	Regular-training	TRADES	GAT	GPGD-AT	RST	PUAT-L	PUAT
Regular-training	—	55.73 ± 6.88	57.04 ± 2.68	65.77 ± 3.15	50.93 ± 5.20	72.18 ± 0.53	<b>76.73 ± 1.44</b>
TRADES	60.88 ± 0.84	—	55.45 ± 3.93	61.71 ± 2.34	45.99 ± 4.41	68.86 ± 0.14	<b>73.37 ± 1.95</b>
GAT	59.47 ± 1.32	43.66 ± 6.54	—	62.20 ± 2.84	47.76 ± 4.04	69.27 ± 1.64	<b>73.79 ± 1.09</b>
GPGD-AT	58.23 ± 1.33	40.92 ± 5.58	54.24 ± 2.68	—	48.06 ± 3.33	67.59 ± 1.09	<b>73.58 ± 3.18</b>
RST	64.51 ± 0.26	47.51 ± 4.66	61.98 ± 3.51	68.32 ± 1.27	—	73.81 ± 0.93	<b>78.06 ± 1.27</b>
PUAT-L	65.65 ± 1.95	48.16 ± 8.76	61.32 ± 3.40	69.91 ± 2.68	54.77 ± 4.80	—	<b>75.44 ± 2.74</b>
PUAT	<b>73.73 ± 1.34</b>	<b>65.18 ± 3.91</b>	<b>72.23 ± 4.08</b>	<b>77.79 ± 2.29</b>	<b>61.37 ± 4.98</b>	<b>79.62 ± 0.76</b>	—

$y_2 = "1"$ ,  $y_3 = "2"$  on SVHN. Then for each  $y_i$ ,  $i = 1, 2, 3$ , we invoke  $G$  to generate a set of  $\{(x_g, y_i)\}$  such that  $|\{(x_g, y_i) \sim P_G(x, y)\}| = |\{(x_l, y_i) \sim P(x, y)\}|$ . At the same time, all the testing examples are also fed into  $C$ , and those classified as  $y_1$ ,  $y_2$  or  $y_3$  make up  $\{(x_c, y_i) \sim P_C(x, y)\}$ . At last, we plot the sample points  $\{(x_l, y_i)\}$ ,

$\{(x_g, y_i)\}$ , and  $\{(x_c, y_i)\}$  ( $i = 1, 2, 3$ ) in Figure 4 by using t-SNE algorithm, where different colors denote classes and different patterns denote distributions.

Figures 4(a) and 4(c) show the results of the complete PUAT on CIFAR10 and SVHN, respectively. From Figures 4(a) and 4(c) we can see that the data points are distributed

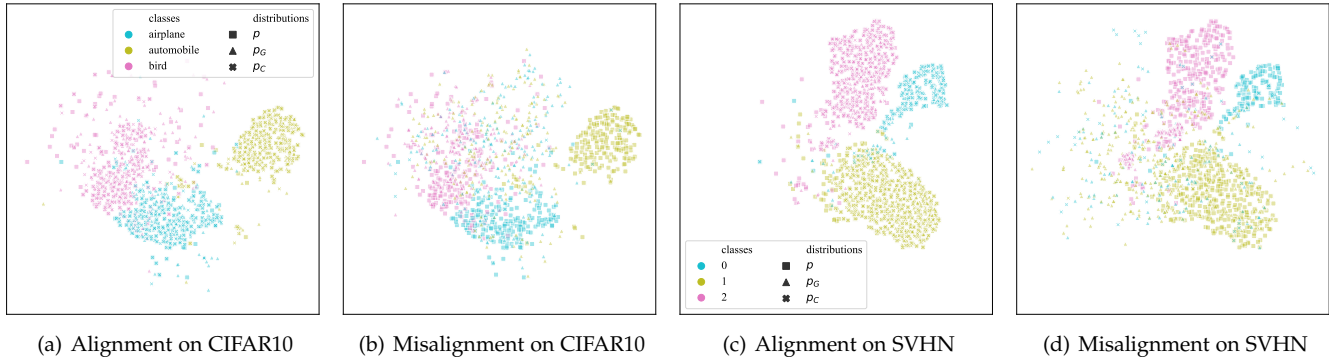


Fig. 4. Visualized distribution alignment or misalignment, where different colors denote classes and different patterns denote distributions.

TABLE 11

The sample number of different classes from different distributions.

Distribution	CIFAR10			SVHN		
	"airplane"	"automobile"	"bird"	"0"	"1"	"2"
$P(y)$	200	200	200	133	391	318
$P_G(y)$	200	200	200	133	391	318
$P_C(y)$	213	203	170	148	338	279
misaligned $P_C(y)$	8	1	42	46	2	0

in three different colored clusters with clear boundaries, where the examples from different distributions (with different patterns) but of the same class (with the same color) are grouped in the same cluster, and there are essentially no data points in any cluster that have a different color from the majority. However, once we remove the extended AT from PUAT so that Theorem 1 does not hold, the cluster boundaries become blurred and the colors in the same cluster become impure, as shown in Figures 4(b) and 4(d). Therefore, we can contend that PUAT aligns the three conditional distributions  $P(x|y)$ ,  $P_C(x|y)$  and  $P_G(x|y)$ . Furthermore, as shown in Table 11, when the distributions are aligned, the number of examples belonging to  $y_i$  is approximately the same in different distributions, which indicates  $P(y) = P_G(y) = P_C(y)$ , so we can confirm that  $P(x, y)$ ,  $P_C(x, y)$  and  $P_G(x, y)$  are aligned by PUAT.

## 6 RELATED WORK

In this section, we briefly introduce the related works from three domains, adversarial attacks, adversarial training, and standard generalizability, and comment their differences from our work.

### 6.1 Adversarial Attacks

Generally, adversarial attacks aim to fool a target model well-trained on natural data with AEs that are imperceptible to humans [4], [34]. The existence of AEs is first discovered by the seminal works of Szegedy *et al.* [2] and Goodfellow *et al.* [8]. In [2], Szegedy *et al.* propose an attack method called L-BFGS which can imperceptibly perturb a natural example with respect to its second-order gradient to cause misclassifications. In [8], Goodfellow *et al.* further propose the fast

gradient sign method (FGSM), which searches adversarial perturbations just based on a single first-order gradient step. Following the idea of [8], various adversarial attack methods have been proposed by enhancing the first-order method. For example, Madry *et al.* [9] propose a projected gradient descent (PGD) method which can be regarded as an iterative FGSM projecting AEs into a ball constrained by  $L_\infty$  norm. Instead of restricting the perturbation norms to a fixed value, Moosavi-Dezfooli *et al.* [35] propose an optimization based attack method Deepfool to seek adversarial perturbations for differentiable classifiers by minimizing  $L_2$  norm. Similarly, Carlini and Wagner [36] propose another optimization based method called C&W attack, which can generate stronger AEs with perturbations minimizing  $L_0$ ,  $L_2$  and  $L_\infty$  norms at the expense of higher computation complexity. In contrast to gradient based methods, another line of works employs GAN to generate AEs for better imperceptibility. For example, Xiao *et al.* [37] propose AdvGAN to generate perturbations for observed examples, which extends standard GAN with explicit perturbation norm loss to ensure the imperceptibility. Additionally, instead of generating an AE by perturbing a single example, Moosavi-Dezfooli *et al.* [38] also further propose universal adversarial perturbations which are computed in an example-agnostic fashion and can fool the target classifier on any examples.

The above-mentioned adversarial attacks focus on the AEs which are generated by adding imperceptible perturbations restricted by  $L_p$  norm on observed examples, which we call restricted AE (RAE). Recently, some researchers have discovered that there exist unrestricted AEs (UAEs) that are norm-constrained. To ensure the imperceptibility of UAEs, one line of UAE generation methods manipulates example features by perturbations within perceptual distances that are aligned with human perception [18], [19], [39], [40]. At the same time, some researchers find that in a broader sense, UAEs can be completely new examples built from scratch and dissimilar to any observed example but can still fool classifiers without confusing humans [16]. Following this idea, a few of UAE generation methods based on generative models are proposed [16], [17], [20], [32], [41], [42]. For example, Song *et al.* [16] and Xiao *et al.* [32] propose to first generate perturbations based on initial random noise and then feed them into a pre-trained conditional GAN (e.g. AC-GAN [43]) to produce UAEs, while Poursaeed *et al.* [41] propose to use a Style-GAN [44] to synthesize UAEs with

stylistic perturbations.

The existing works for UAE generation, however, do not explain why UAEs pose threats, or rather, where the imperceptibility of UAEs stems. By contrast, our work proposes a novel viewpoint to view UAEs as perturbed unobserved examples, which provides a logical and provable explanation of UAE's dissimilarity to observed examples, imperceptibility to humans, and the feasibility of comprehensive adversarial robustness. Based on this understanding, we further propose a novel G-C-D GAN for UAE generation, which together with the attacker  $A$  can synthesize UAEs that are more adversarial by aligning UAE distribution with natural data distribution.

## 6.2 Adversarial Training

AT has proved to be the strongest principled defensive technique against adversarial attacks [5], [6], [7]. The basic idea of AT is initially proposed by Szegedy *et al.* [2], which uses a min-max game to incorporate deliberately crafted AEs to the training process of a DNN model to obtain immunity against AEs. Madry *et al.* [9] are the first time to theoretically justify the adversarial robustness offered by the min-max optimization used in AT.

Over the past few years, many enhancements of AT have been proposed to employ various perturbation generation methods to improve adversarial robustness [10], [11], [12], [13], [14], [15]. For example, Wang *et al.* [10] propose a bilateral adversarial training method that perturbs both normal images and real labels with respect to a smaller gradient magnitude. Wang *et al.* [11] propose a misclassification-aware adversarial training (MART) method, which defines a novel adversarial loss with a regularization on misclassified examples. Cheng *et al.* [12] argue that large perturbations may be more adversarial for the robustness of a target model and propose a customized adversarial training (CAT) method which can offer adaptive perturbations for natural examples. Shafahi *et al.* [13] propose a universal adversarial training method for the robustness against universal attacks [38]. Among others, generative model-based AT methods are verified as a promising approach due to the GAN's capability of distributional alignment. For example, to strengthen the adversaries, Lee *et al.* [14] propose a generative adversarial trainer (GAT) which employs a GAN to produce adversarial perturbations with respect to the gradients of the natural examples, while Stutz *et al.* [15] propose to use VAE-GAN to produce AEs whose distribution is aligned with that of the natural examples. As discussed in 6.1, GAN-based methods strengthen AEs with stronger imperceptibility because of the alignment between the distributions of AEs and the natural examples, which is equivalent to drawing AEs on the manifold (distribution) of the natural examples.

The above-mentioned AT methods are basically based on supervised learning, which often suffer from the sparsity of labeled data. Recently, some researchers have discovered that introducing richer unlabeled data can increase the performance of AT, and hence proposed semi-supervised AT methods leveraging partially labeled data [33], [45], [46]. For example, Zhang *et al.* [45] argue that the performance of AT will be impaired by the perturbations generated only based on labeled data since they are unable to reflect the underlying distribution of all potential examples, and propose

a GAN-based semi-supervised AT method where AEs can preserve the inner structure of unlabeled data. Carmon *et al.* [33] propose a robust self-training (RST) model which first uses an intermediate classifier trained on labeled examples to infer the labels for the unlabeled examples, and then generate AEs for AT from the labeled and pseudo-labeled examples. Stanforth *et al.* [46] propose an unsupervised adversarial training (UAT) method which estimates the worst-case AEs with KL-divergence between the distributions of the perturbed unlabeled examples and the natural unlabeled examples.

However, the AEs used in traditional AT methods are generated by adding norm-bounded perturbations, even though which are generated by GAN, to observed examples, which limits traditional AT methods to providing only the adversarial robustness against RAEs. To overcome this limitation, recently, Xiao *et al.* [32] propose a new AT method called GPGD-AT, which conducts AT over UAEs generated by their GPGD. In particular, GPGD first employs a conditional GAN to generate an unobserved labeled example, then adds adversarial perturbation to it based on the gradient of the target classifier loss incurred by the generated example. However, as the problem of UAE generation, AT on UAEs still remains under-explored.

Different from the existing AT methods providing adversarial robustness against either RAE or UAE, our PUAT focuses on the concept of generalized UAE which makes it feasible to offer comprehensive adversarial robustness against both UAE and RAE. At the same time, PUAT is both GAN-based and semi-supervised, which improves the AT performance with stronger UAEs compared with GPGD-AT.

## 6.3 Standard Generalizability

A model's standard generalizability and adversarial robustness are measured by its accuracy on testing natural examples and testing AEs, respectively. Traditional AT methods are based on AEs with norm-constraints, which will lead to distribution-shift between AEs and natural examples [32], [47]. Therefore, there is a belief that AT forces the target model to generalize on two separated distributions and hence the tradeoff between standard generalizability and adversarial robustness inevitably comes into being, or in other words, adversarial robustness comes at the expense of standard generalizability [9], [21], [31], [47].

However, some researchers have opposing opinions that the tradeoff may be not inevitable, with support of recent empirical evidences and theoretical analyses [15], [23], [24], [25], [48]. One line of works tries to extend the existing AT methods with regularizations to mitigate the tradeoff. For example, Song *et al.* [24] and Xing *et al.* [25] propose to improve the generalizability by introducing robust local features and  $l_1$  penalty to AT, respectively. The other line aims at breaking the tradeoff by exploiting the distributional property of AEs and natural examples. For example, Yang *et al.* [23] discover the  $r$ -separation phenomenon in widely-used image datasets, namely the distributions of different classes are at least distance  $2r$  apart from each other in pixel space. Based on this discovery, they theoretically prove that a classifier with sufficient local Lipschitz smoothness can achieve both high accuracy on natural examples and

acceptable robustness on AEs with perturbations of size up to  $r$ . Differently, Stutz *et al.* [15] find that there exist AEs on the manifold of natural examples, and hence the adversarial robustness against the on-manifold AEs will equivalently improve the standard generalizability. Similarly, Staib *et al.* [48] propose Distributionally Robust Optimization (DRO), which offers a more general perspective that the tradeoff can be eliminated by the alignment between the distributions of AEs and natural examples. Instead of generating point-wise perturbations with norm-constrained magnitude, DRO aims to seek worst-case AE distribution by restricting the distance between the AE distribution  $\tilde{p}$  and the natural data distribution  $p$  through the following min-max game:

$$\min_C \max_{\tilde{P}(\tilde{x}, y): W_p(P, \tilde{P}) \leq \epsilon} \mathbb{E}_{P(x, y)} [\mathcal{L}(C(\tilde{x}), y)],$$

where  $W_p$  is a distributional distance measure, e.g., Wasserstein distance. As  $\epsilon$  approaching 0,  $\tilde{P}$  is gradually aligning with  $P$ , and consequently, the tradeoff tends to disappear. Indeed, on-manifold AEs can be seen as a special case of DRO when  $\epsilon = 0$ .

Our work provides new arguments for the opinion that the tradeoff is eliminable. In particular, we make two contributions which distinguish our work from the existing works addressing the tradeoff: (1) We extend the research scope to UAEs by proposing a novel AT method PUAT; (2) By solid theoretical analysis and extensive empirical investigation, we show that the standard generalizability and comprehensive adversarial robustness are both achievable for PUAT.

## 7 CONCLUSION

In this paper, we propose a unique viewpoint that understands UAEs as imperceptibly perturbed unobserved examples, which rationalizes why UAEs exist and why they are able to deceive a well-trained classifier. This understanding allows us to view RAE as a special UAE, thus providing the feasibility of achieving comprehensive adversarial robustness against both UAE and RAE. Also, we find that if the UAE distribution and the natural data distribution can be aligned, the conflict between robust generalization and standard generalization in traditional AT methods can be eliminated, thus improving both the adversarial robustness and standard generalizability of a target classifier. Based on these ideas, we propose a novel AT method called Provable Unrestricted Adversarial Training (PUAT). PUAT utilizes partially labeled data to achieve efficient UAE generation by accurately capturing the real data distribution through a well-designed G-C-D GAN. At the same time, PUAT extends the traditional AT by introducing the supervised loss of the target classifier into the adversarial training and achieves alignment between the UAE distribution, the natural data distribution, and the distribution learned by the classifier, with the collaboration of the G-C-D GAN. The solid theoretical analysis and the extensive experiments demonstrate that PUAT can eliminate tradeoffs between adversarial robustness and standard generalizability through distributional alignment, and compared to the baseline methods, PUAT enables a target classifier to better defend against both UAE attacks and RAE attacks, as well as significantly increases its standard generalizability.

## ACKNOWLEDGMENTS

This work is supported by National Natural Science Foundation of China under grant 61972270, and in part by NSF under grants III-1763325, III-1909323, III-2106758, and SaTC-1930941.

## REFERENCES

- [1] B. Biggio, I. Corona, D. Maiorca, B. Nelson, N. Šrncić, P. Laskov, G. Giacinto, and F. Roli, "Evasion attacks against machine learning at test time," in *Joint European Conference on Machine Learning and Knowledge Discovery in Databases*, 2013, pp. 387–402.
- [2] C. Szegedy, W. Zaremba, I. Sutskever, J. Bruna, D. Erhan, I. Goodfellow, and R. Fergus, "Intriguing properties of neural networks," in *International Conference on Learning Representations*, 2014.
- [3] A. Ilyas, S. Santurkar, D. Tsipras, L. Engstrom, B. Tran, and A. Madry, "Adversarial examples are not bugs, they are features," *Advances in Neural Information Processing Systems*, vol. 32, 2019.
- [4] D. J. Miller, Z. Xiang, and G. Kesidis, "Adversarial learning targeting deep neural network classification: A comprehensive review of defenses against attacks," *Proceedings of the IEEE*, vol. 108, no. 3, pp. 402–433, 2020.
- [5] T. Bai, J. Luo, J. Zhao, B. Wen, and Q. Wang, "Recent advances in adversarial training for adversarial robustness," in *Proceedings of the Thirtieth International Joint Conference on Artificial Intelligence (IJCAI-21)*, 2021.
- [6] N. Akhtar, A. Mian, N. Kardan, and M. Shah, "Advances in adversarial attacks and defenses in computer vision: A survey," *IEEE Access*, vol. 9, pp. 155 161–155 196, 2021.
- [7] W. Zhao, S. Alwidian, and Q. H. Mahmoud, "Adversarial training methods for deep learning: A systematic review," *Algorithms*, vol. 15, no. 8, p. 283, 2022.
- [8] I. J. Goodfellow, J. Shlens, and C. Szegedy, "Explaining and harnessing adversarial examples," in *International Conference on Learning Representations*, 2014.
- [9] A. Madry, A. Makelov, L. Schmidt, D. Tsipras, and A. Vladu, "Towards deep learning models resistant to adversarial attacks," in *International Conference on Learning Representations*, 2018.
- [10] J. Wang and H. Zhang, "Bilateral adversarial training: Towards fast training of more robust models against adversarial attacks," in *Proceedings of the IEEE/CVF International Conference on Computer Vision*, 2019.
- [11] Y. Wang, D. Zou, J. Yi, J. Bailey, X. Ma, and Q. Gu, "Improving adversarial robustness requires revisiting misclassified examples," in *International Conference on Learning Representations*, 2020.
- [12] M. Cheng, Q. Lei, P.-Y. Chen, I. Dhillon, and C.-J. Hsieh, "Cat: Customized adversarial training for improved robustness," *CoRR*, vol. abs/2002.06789, 2020.
- [13] A. Shafahi, M. Najibi, Z. Xu, J. Dickerson, L. S. Davis, and T. Goldstein, "Universal adversarial training," in *Proceedings of the AAAI Conference on Artificial Intelligence*, vol. 34, no. 04, 2020, pp. 5636–5643.
- [14] H. Lee, S. Han, and J. Lee, "Generative adversarial trainer: Defense to adversarial perturbations with gan," *CoRR*, vol. abs/1705.03387, 2017.
- [15] D. Stutz, M. Hein, and B. Schiele, "Disentangling adversarial robustness and generalization," in *Proceedings of the IEEE/CVF Conference on Computer Vision and Pattern Recognition*, 2019, pp. 6976–6987.
- [16] Y. Song, R. Shu, N. Kushman, and S. Ermon, "Constructing unrestricted adversarial examples with generative models," *Advances in Neural Information Processing Systems*, vol. 31, 2018.
- [17] I. Dunn, H. Pouget, T. Melham, and D. Kroening, "Adaptive generation of unrestricted adversarial inputs," *CoRR*, vol. abs/1905.02463, 2019.
- [18] A. Bhattad, M. J. Chong, K. Liang, B. Li, and D. A. Forsyth, "Unrestricted adversarial examples via semantic manipulation," in *International Conference on Learning Representations*, 2020.
- [19] H. Naderi, L. Goli, and S. Kasaei, "Generating unrestricted adversarial examples via three parameters," *Multimedia Tools and Applications*, pp. 1–20, 2022.
- [20] T. Xiang, H. Liu, S. Guo, Y. Gan, and X. Liao, "Egm: An efficient generative model for unrestricted adversarial examples," *ACM Transactions on Sensor Networks*, 2022.

- [21] D. Tsipras, S. Santurkar, L. Engstrom, A. Turner, and A. Madry, "Robustness may be at odds with accuracy," in *International Conference on Learning Representations*, 2019.
- [22] I. Attias, A. Kontorovich, and Y. Mansour, "Improved generalization bounds for adversarially robust learning," *Journal of Machine Learning Research*, vol. 23, no. 175, pp. 1–31, 2022.
- [23] Y.-Y. Yang, C. Rashtchian, H. Zhang, R. R. Salakhutdinov, and K. Chaudhuri, "A closer look at accuracy vs. robustness," *Advances in Neural Information Processing Systems*, vol. 33, 2020.
- [24] C. Song, K. He, J. Lin, L. Wang, and J. E. Hopcroft, "Robust local features for improving the generalization of adversarial training," in *International Conference on Learning Representations*, 2020.
- [25] Y. Xing, Q. Song, and G. Cheng, "On the generalization properties of adversarial training," in *International Conference on Artificial Intelligence and Statistics*. PMLR, 2021, pp. 505–513.
- [26] C. Li, T. Xu, J. Zhu, and B. Zhang, "Triple generative adversarial nets," *Advances in Neural Information Processing Systems*, vol. 30, 2017.
- [27] C. Li, K. Xu, J. Zhu, J. Liu, and B. Zhang, "Triple generative adversarial networks," *IEEE Transactions on Pattern Analysis and Machine Intelligence*, vol. 44, no. 12, pp. 9629–9640, 2022.
- [28] I. J. Goodfellow, J. Pouget-Abadie, M. Mirza, B. Xu, D. Warde-Farley, S. Ozair, A. C. Courville, and Y. Bengio, "Generative adversarial nets," in *Advances in Neural Information Processing Systems*, 2014.
- [29] A. Krizhevsky, "Learning multiple layers of features from tiny images," *CiteSeer*, 2009.
- [30] Y. Netzer, T. Wang, A. Coates, A. Bissacco, B. Wu, and A. Y. Ng, "Reading digits in natural images with unsupervised feature learning," in *Advances in Neural Information Processing Systems Workshop on Deep Learning and Unsupervised Feature Learning*, 2011.
- [31] H. Zhang, Y. Yu, J. Jiao, E. Xing, L. El Ghaoui, and M. Jordan, "Theoretically principled trade-off between robustness and accuracy," in *International Conference on Machine Learning*. PMLR, 2019, pp. 7472–7482.
- [32] J. Xiao, L. Yang, Y. Fan, J. Wang, and Z.-Q. Luo, "Understanding adversarial robustness against on-manifold adversarial examples," *CoRR*, vol. abs/2210.00430, 2022.
- [33] Y. Carmon, A. Raghunathan, L. Schmidt, J. C. Duchi, and P. S. Liang, "Unlabeled data improves adversarial robustness," in *Advances in Neural Information Processing Systems*, 2019.
- [34] X. Zhang, X. Zheng, and W. Mao, "Adversarial perturbation defense on deep neural networks," *ACM Computing Surveys (CSUR)*, vol. 54, no. 8, pp. 1–36, 2021.
- [35] S.-M. Moosavi-Dezfooli, A. Fawzi, and P. Frossard, "Deepfool: a simple and accurate method to fool deep neural networks," in *Proceedings of the IEEE conference on computer vision and pattern recognition*, 2016.
- [36] N. Carlini and D. Wagner, "Towards evaluating the robustness of neural networks," in *2017 IEEE Symposium on Security and Privacy (SP)*, 2017, pp. 39–57.
- [37] C. Xiao, B. Li, J.-Y. Zhu, W. He, M. Liu, and D. Song, "Generating adversarial examples with adversarial networks," *CoRR*, vol. abs/1801.02610, 2018.
- [38] S.-M. Moosavi-Dezfooli, A. Fawzi, O. Fawzi, and P. Frossard, "Universal adversarial perturbations," in *Proceedings of the IEEE conference on computer vision and pattern recognition*, 2017.
- [39] A. S. Shamsabadi, R. Sanchez-Matilla, and A. Cavallaro, "Colorfool: Semantic adversarial colorization," in *Proceedings of the IEEE/CVF Conference on Computer Vision and Pattern Recognition*, 2020, pp. 1151–1160.
- [40] Z. Zhao, Z. Liu, and M. Larson, "Towards large yet imperceptible adversarial image perturbations with perceptual color distance," in *Proceedings of the IEEE/CVF Conference on Computer Vision and Pattern Recognition*, 2020.
- [41] O. Poursaeed, T. Jiang, Y. Goshu, H. Yang, S. Belongie, and S.-N. Lim, "Fine-grained synthesis of unrestricted adversarial examples," *CoRR*, vol. abs/1911.09058, 2019.
- [42] X. Wang, K. He, and J. E. Hopcroft, "At-gan: A generative attack model for adversarial transferring on generative adversarial nets," *CoRR*, vol. abs/1904.07793, 2019.
- [43] A. Odena, C. Olah, and J. Shlens, "Conditional image synthesis with auxiliary classifier gans," in *International Conference on Machine Learning*. PMLR, 2017, pp. 2642–2651.
- [44] T. Karras, S. Laine, and T. Aila, "A style-based generator architecture for generative adversarial networks," in *Proceedings of the IEEE/CVF conference on computer vision and pattern recognition*, 2019.
- [45] H. Zhang and J. Wang, "Defense against adversarial attacks using feature scattering-based adversarial training," in *Advances in Neural Information Processing Systems*, 2019.
- [46] J.-B. Alayrac, J. Uesato, P.-S. Huang, A. Fawzi, R. Stanforth, and P. Kohli, "Are labels required for improving adversarial robustness?" in *Advances in Neural Information Processing Systems*, 2019.
- [47] S. Yang, T. Guo, Y. Wang, and C. Xu, "Adversarial robustness through disentangled representations," in *Proceedings of the AAAI Conference on Artificial Intelligence*, 2021.
- [48] M. Staib and S. Jegelka, "Distributionally robust deep learning as a generalization of adversarial training," in *NIPS workshop on Machine Learning and Computer Security*, 2017.



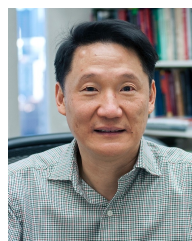
**Lilin Zhang** obtained her bachelor's degree from the School of Information and Security Engineering, Zhongnan University of Economics and Law, in 2021. She is now pursuing the master's degree in the School of Computer Science, Sichuan University, China. Her research interest focuses on adversarial machine learning and its applications.



**Ning Yang** is an associate professor at Sichuan University, China. He obtained his PhD degree in Computer Science from Sichuan University in 2010. His research interests include adversarial machine learning, graph learning, and recommender systems.



**Yanchao Sun** is a Ph.D. candidate in University of Maryland, College Park, USA, where she is advised by Prof. Furong Huang. Her research mainly focuses on reinforcement learning (RL), including adversarial RL, multi-task RL, sample-efficient RL, etc.



**Philip S. Yu** received the PhD degree in electrical engineering from Stanford University. He is a distinguished professor in computer science at the University of Illinois at Chicago and is also the Wexler chair in information technology. His research interests include big data, data mining, and social computing. He is a fellow of the ACM and the IEEE.